

Article

Biomechanical Posture Analysis in Healthy Adults with Machine Learning: Applicability and Reliability

Federico Roggio ¹, Sarah Di Grande ², Salvatore Cavalieri ², Deborah Falla ³ and Giuseppe Musumeci ^{1,4,5,*}

- ¹ Department of Biomedical and Biotechnological Sciences, Section of Anatomy, Histology and Movement Science, School of Medicine, University of Catania, Via S. Sofia n°97, 95123 Catania, Italy; federico.roggio@unict.it
- ² Department of Electrical Electronic and Computer Engineering, University of Catania, Viale A. Doria 6, 95125 Catania, Italy; sarah.digrande@phd.unict.it (S.D.G.); salvatore.cavalieri@unict.it (S.C.)
- ³ Centre of Precision Rehabilitation for Spinal Pain (CPR Spine), School of Sport, Exercise and Rehabilitation Sciences, University of Birmingham, Birmingham B15 2TT, UK; d.falla@bham.ac.uk
- ⁴ Research Center on Motor Activities (CRAM), University of Catania, Via S. Sofia n°97, 95123 Catania, Italy
- ⁵ Department of Biology, Sbarro Institute for Cancer Research and Molecular Medicine, College of Science and Technology, Temple University, Philadelphia, PA 19122, USA
- * Correspondence: g.musumeci@unict.it

Abstract: Posture analysis is important in musculoskeletal disorder prevention but relies on subjective assessment. This study investigates the applicability and reliability of a machine learning (ML) pose estimation model for the human posture assessment, while also exploring the underlying structure of the data through principal component and cluster analyses. A cohort of 200 healthy individuals with a mean age of 24.4 ± 4.2 years was photographed from the frontal, dorsal, and lateral views. We used Student's *t*-test and Cohen's effect size (*d*) to identify gender-specific postural differences and used the Intraclass Correlation Coefficient (ICC) to assess the reliability of this method. Our findings demonstrate distinct sex differences in shoulder adduction angle (men: $16.1^\circ \pm 1.9^\circ$, women: $14.1^\circ \pm 1.5^\circ$, *d* = 1.14) and hip adduction angle (men: $9.9^\circ \pm 2.2^\circ$, women: $6.7^\circ \pm 1.5^\circ$, *d* = 1.67), with no significant differences in horizontal inclinations. ICC analysis, with the highest value of 0.95, confirms the reliability of the approach. Principal component and clustering analyses revealed potential new patterns in postural analysis such as significant differences in shoulder–hip distance, highlighting the potential of unsupervised ML for objective posture analysis, offering a promising non-invasive method for rapid, reliable screening in physical therapy, ergonomics, and sports.

Keywords: biomechanics; machine learning; posture analysis; reliability; principal component analysis; cluster analysis; musculoskeletal disorders; ergonomics; kinesiology



Citation: Roggio, F.; Di Grande, S.; Cavalieri, S.; Falla, D.; Musumeci, G. Biomechanical Posture Analysis in Healthy Adults with Machine Learning: Applicability and Reliability. *Sensors* **2024**, *24*, 2929. <https://doi.org/10.3390/s24092929>

Academic Editor: Christian Peham

Received: 8 April 2024

Revised: 30 April 2024

Accepted: 2 May 2024

Published: 4 May 2024



Copyright: © 2024 by the authors. Licensee MDPI, Basel, Switzerland. This article is an open access article distributed under the terms and conditions of the Creative Commons Attribution (CC BY) license (<https://creativecommons.org/licenses/by/4.0/>).

1. Introduction

The structure and function of the body provide the potential for achieving and maintaining an appropriate posture; however, the persistence of poor postural habits can lead to discomfort, pain, or disability [1]. Many methods are available to evaluate posture, each of them with strengths and weaknesses [2]. Optoelectronic motion capture systems are considered the gold standard for human movement analysis [3], although they are expensive and commonly limited to laboratory environments. On the other hand, smartphone applications are low-cost and portable [4,5], but their reliability may be lower [2].

Artificial Intelligence (AI), particularly machine learning (ML), has revolutionized healthcare data analysis [6], supporting the diagnosis of various conditions like gait disorders [7], Parkinson's disease [8], stroke [9], and osteoarthritis [10]. Traditional human motion analysis methods are rapidly evolving due to advancements in ML and computer vision. For example, previous studies have explored ML models for identifying postural abnormalities in Parkinson's disease patients using Microsoft Kinect data [11]. The development of sophisticated pose estimation models has revolutionized anatomical landmark

extraction from images and videos, enabling a new era of ML-driven movement analysis. However, applying ML human pose estimation models specifically for posture assessment remains a relatively unexplored area [12]. Traditional posture assessment methods often suffer from subjectivity and low reliability due to visual inspection [13]. This inconsistency underscores the need for an objective, AI-driven method that minimizes clinician bias, which is crucial given the role of posture in musculoskeletal disorder prevention [14]. This presents a significant opportunity for innovative research in this field [12]. Recently, many digital alternatives have emerged as accessible methods for human pose estimation, such as MediaPipe [15], OpenPose [16], MoveNet [17], and PoseNet [18]. Their strength lies in the possibility of performing objective and reproducible analyses with a simple video or photo achieved in any environment [19,20]. Such methods are being employed in different scenarios. For example, while traditional ergonomic risk assessment often relies on human observation, recent ML-based methods have demonstrated the value of analyzing a worker's musculoskeletal load based on relative body part positions, highlighting their applicability in work-related scenarios [21]. Additionally, previous research has compared the effectiveness of OpenPose for gait analysis directly with marker-based motion capture systems. This study concluded that the ML approach outperformed traditional methods, demonstrating its potential as a cost-efficient alternative for video analysis in out-of-laboratory environments [22]. Furthermore, studies using OpenPose have shown promising results in applying a deep learning pipeline to differentiate neurological gait patterns between Parkinson's disease and multiple sclerosis [23]. The development of in-home gait monitoring tools could be a valuable resource for both diagnosis and clinician support in telemedicine systems.

MediaPipe Pose is a powerful ML algorithm from the Google research team, designed to accurately track human body poses. It estimates 33 landmarks across the body from 2D photos or videos, enabling detailed motion tracking by determining their 3D positions [24,25]. To ensure the accuracy of its 3D pose estimations, MediaPipe uses ground truth data obtained through a statistical 3D human body model (GHUM), built using a large dataset of human shapes and motions [26]. This model is then fitted to 2D pose data and further refined with real-world 3D keypoint coordinates. During this process, the shape and pose variables of the GHUM are optimized to align with image evidence for maximum precision. The validity of the MediaPipe joint inference tracking technique has been thoroughly investigated. Lafayette et al. [27] conducted a quantitative evaluation of its angular estimation capabilities by comparing it to a gold-standard Qualisys motion capture system [28]. They found an excellent absolute relative clinical error and a strong correlation with Qualisys, with mean Pearson's coefficients of 0.80 and 0.91 for lower and upper limb movements. Further validation studies on MediaPipe performance come from its ability to categorize exercise postures with 100% precision [29] and detect human movements in non-standard videos with over 90% accuracy [30].

Principal component analysis (PCA) is a powerful dimensionality reduction technique widely used in machine learning and movement analysis [31,32]. It offers a non-reductionist approach to biomechanics, minimizing investigator bias and enriching the understanding of body part interactions [32,33]. Clustering analysis is another valuable method for discovering new patterns in multidimensional data by organizing them into clusters based on similarities [34]. It has applications in biomechanics, including gait analysis [35], movement kinematics [36], and injury prevention [37]. The rationale for using ML algorithms like PCA and cluster analysis in posture assessment lies in their ability to analyze high-dimensional data, revealing patterns and relationships that might be overlooked by traditional methods.

The significant potential of these ML approaches makes their transition into clinical settings crucial, especially considering the limited number of studies that have attempted this to date [19,38]. Therefore, the aim of the current study is two-fold. First, it aims to demonstrate the applicability and reliability of an ML approach for analyzing posture, with the goal of providing normative data on healthy men and women. Subsequently, it aims to offer new insights into posture by applying PCA and clustering methods to the data. This dual approach aims to enhance the depth of posture analysis in the clinical context.

2. Materials and Methods

For this cross-sectional study, a total of 250 volunteers were initially recruited at the Research Center on Motor Activities (CRAM) of the University of Catania, Italy, from March 2023 to June 2023. After applying exclusion criteria for musculoskeletal and neurological pathologies, or musculoskeletal trauma within the past six months, 200 healthy participants, consisting of 84 men and 116 women, were included, aged between 18 and 30 years (mean age 24.4 ± 4.2 years). Participants were requested to wear minimal clothing, such as shorts and a t-shirt for men, or a sports bra and shorts for women. The required sample size was calculated using G*Power. To ensure adequate statistical power and account for potential data loss, we aimed for a slightly larger sample size from 176 to 200 participants.

Photos were collected while the participants adopted the anatomical zero position [39]; this involved standing upright, facing forward, with arms resting at their sides, hands facing the body, and forearms midway between supination and pronation. The feet were aligned, spaced 10 cm apart, and positioned at a 20° total out-toeing angle. They were asked to stand still 1.5 m distant from a smartphone with a 50 MP 1/1.56" sensor camera mounted on a tripod while collecting the photos. Each measurement was collected in the morning, from 9 a.m. to 12 a.m. To ensure the reliability of the study, a subgroup of 90 participants underwent the same procedure after one week. This study received approval from the Scientific Committee of the University of Catania's Research Center on Motor Activities (Protocol n.: CRAM-035-2023, 15 March 2023), and was conducted in accordance with the Declaration of Helsinki. Participants signed written informed consent forms to agree to participate in the study.

2.1. Pose Estimation

A total of 33 anatomical landmarks were predicted using MediaPipe Pose with a BlazePose and MobileNetv2 Convolutional Neural Network architecture [40]. This model detects human bodies, analyzes images, produces heatmaps and offsets, and identifies body landmarks, as shown in Figure 1. Body orientation is determined automatically by identifying the hip midpoint and the angle of the shoulder–hip line. To obtain 3D projections of each anatomical landmark, we extracted their x, y, and z coordinates; then, we calculated joint angles between body segments using the circular mean of data from frontal and dorsal photos to improve accuracy. Further, we determined vertical and horizontal inclinations of vectors between landmarks. Body vector lengths were calculated as distances between landmarks, e.g., shoulder–elbow, using pixel distance (pd) as measurement unit. The lateral photo was used for neck and trunk inclinations. For detailed calculation methods, refer to Table A1.

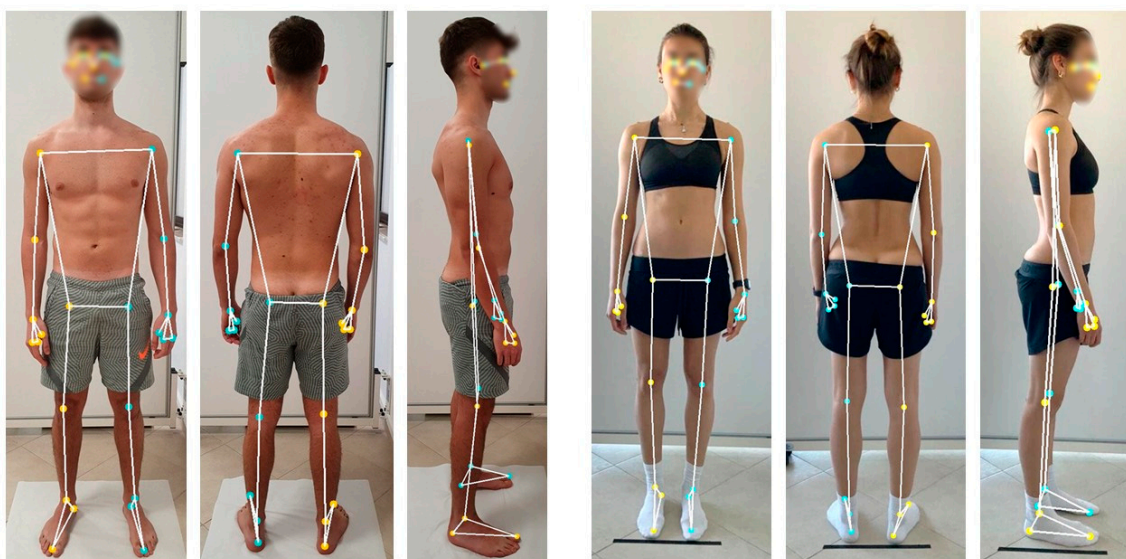


Figure 1. Pose estimation of the collected photos, visualization of the superimposed skeletal model highlighting the anatomical landmarks on frontal, dorsal, and lateral photo views of a woman and a man.

2.2. Data Analysis

The data underwent three layers of analysis. We used Python for building our algorithm model and R Project for Statistical Computing (Vienna, Austria) for the statistical analyses. The Shapiro–Wilk test verified the normality of the data, while Student’s *t*-test and Mann–Whitney U test identified any significant differences between men and women, considering results with a *p*-value < 0.05 to be significant. Cohen’s *d* measured the effect size between the two groups. Pearson’s correlation coefficient (*r*) assessed the association between height and postural variables, considering relevant only the results with *p*-value < 0.05 and *r* > 0.45. Then, we used the Intraclass Correlation Coefficient (ICC) (3,k) to assess the reliability of this method, along with the Standard Error of Measurement (SEM) and Minimal Detectable Change (MDC).

2.3. Principal Component and Clustering Analyses Methods

We conducted multivariate statistical techniques to examine whether the results could highlight other specific patterns within the sample. Given the presence of 23 variables (see Table A1 for full details), PCA was utilized to reduce dimensionality by transforming correlated variables into uncorrelated principal components, maximizing the explained variance with each component. After conducting PCA, we applied the clustering algorithms, k-means, mean-shift, Ward’s method, complete linkage, and average linkage, to identify natural groupings within the data. The rationale for employing a variety of methods was to ensure a comprehensive exploration of the dataset to determine the strengths of each technique and observe different patterns and relationships within the data. The silhouette score was used to assess the quality of the clustering algorithms.

3. Results

The acquired postural parameters, representing the circular mean of 3D landmarks from frontal and dorsal photos (Table 1, Figure 2), showed significant differences between men and women. Significant anthropometric differences were observed between men and women for age (*p* < 0.05), height (*p* < 0.001), and weight (*p* < 0.001). Men had a mean age of 25.9 ± 5.2 years, a mean body weight of 68.2 ± 10.8 kg, and a mean height of 175 ± 6.4 cm. Women had a mean age of 24.1 ± 4.8 years, a mean body weight of 54.4 ± 3.9 kg, and a mean height of 163 ± 6.1 cm. Notable differences were found in shoulder adduction, elbow extension, hip adduction/extension, and ankle flexion, but not knee flexion or varus/valgus angles. The greatest effect size was observed for hip adduction *d* = 1.67, and the smallest for knee extension *d* = 0.01. The greatest effect size for vertical inclinations was in trunk forward inclination (*d* = 0.66), with no significant difference in leg inclination. No significant differences or large effect sizes were observed in horizontal inclinations. Finally, all vectors showed statistical significance with a large effect size. The shoulder–hip difference demonstrated a valuable effect size of *d* = 1.44. Concerning the correlation analysis, we observed a significant association between height and posture specifically for the following variables: torso vector (*r* = 0.60, *p* < 0.001), total arm vector (*r* = 0.496, *p* < 0.001), total leg vector (*r* = 0.530, *p* < 0.001), and shoulder–hip difference (*r* = 0.473, *p* < 0.001).

Table 1. Results of the postural analysis using ML algorithms with sex differences and test–retest reliability.

	Postural Parameters	Mean ± SD		Sig.	Effect Size (d)	ICC	SEM	MDC
		Men	Women					
Body joints (°)	Shoulder adduction angle	16.1 ± 1.9	14.1 ± 1.5	<0.001 ***	1.14	0.94	0.22	0.61
	Elbow extension angle	7.6 ± 3.6	4.4 ± 2.1	<0.001 ***	1.07	0.93	0.60	1.67
	Hip adduction angle	9.9 ± 2.2	6.7 ± 1.5	<0.001 ***	1.67	0.95	0.16	0.45
	Hip extension angle	3.4 ± 2.3	2.5 ± 1.7	0.005 **	0.50	0.78	0.81	2.25
	Knee varus/valgus angle	2.6 ± 1.0	2.2 ± 0.9	0.027 *	0.39	0.93	0.17	0.44
	Knee extension angle	2.7 ± 1.7	2.7 ± 1.8	0.906	0.01	0.84	0.68	1.89
	Ankle flexion angle	68.6 ± 5.3	72.9 ± 4.9	<0.001 ***	−0.85	0.85	0.67	1.85

Table 1. Cont.

	Postural Parameters	Mean \pm SD		Sig.	Effect Size (d)	ICC	SEM	MDC
		Men	Women					
Horizontal inclinations ($^{\circ}$)	Ear line	2.0 \pm 1.5	2.0 \pm 1.2	0.550	0.02	0.79	0.49	1.38
	Shoulder line	1.2 \pm 0.7	1.2 \pm 0.9	0.740	−0.01	0.73	0.48	1.33
	Elbow line	1.2 \pm 0.9	1.3 \pm 0.9	0.530	−0.12	0.85	0.33	0.93
	Wrist line	1.3 \pm 0.9	1.5 \pm 0.9	0.408	−0.13	0.83	0.34	0.95
	Hip line	1.2 \pm 0.8	1.5 \pm 1.0	0.071	−0.34	0.84	0.36	1.01
	Knee line	2.2 \pm 1.3	2.1 \pm 1.4	0.692	0.04	0.67	0.83	2.30
	Ankle line	1.9 \pm 1.4	2.0 \pm 1.3	0.581	−0.08	0.80	0.67	1.87
Vertical inclinations ($^{\circ}$)	Neck inclination	13.6 \pm 3.2	15.4 \pm 3.3	<0.001 ***	−0.55	0.93	0.89	2.47
	Trunk forward inclination	2.3 \pm 1.4	1.5 \pm 1.1	<0.001 ***	0.66	0.77	0.43	1.20
	Body imbalance	0.9 \pm 0.4	1.3 \pm 0.6	<0.001 ***	−0.64	0.90	0.12	0.35
	Leg inclination	1.8 \pm 0.6	1.8 \pm 0.6	0.547	−0.09	0.80	0.23	0.64
Vectors length (pd)	Shoulder–hip difference	83.8 \pm 14.9	63.4 \pm 13.3	<0.001 ***	1.44			
	Torso vector	292.3 \pm 26.3	244.7 \pm 29.5	<0.001 ***	1.71			
	Total arm vector	297.5 \pm 33.4	257.3 \pm 32.9	<0.001 ***	1.21			
	Total leg vector	388.7 \pm 32.4	358.2 \pm 32.4	<0.001 ***	0.94			

SD = Standard deviation, pd = pixel distance. Significance levels: * $p < 0.05$, ** $p < 0.01$, *** $p < 0.001$. Cohen's d : >0.50 = medium effect size, >0.80 = large effect size. ICC = intraclass correlation coefficient (3,k). SEM = standard error of the mean. MDC = minimum detectable change.

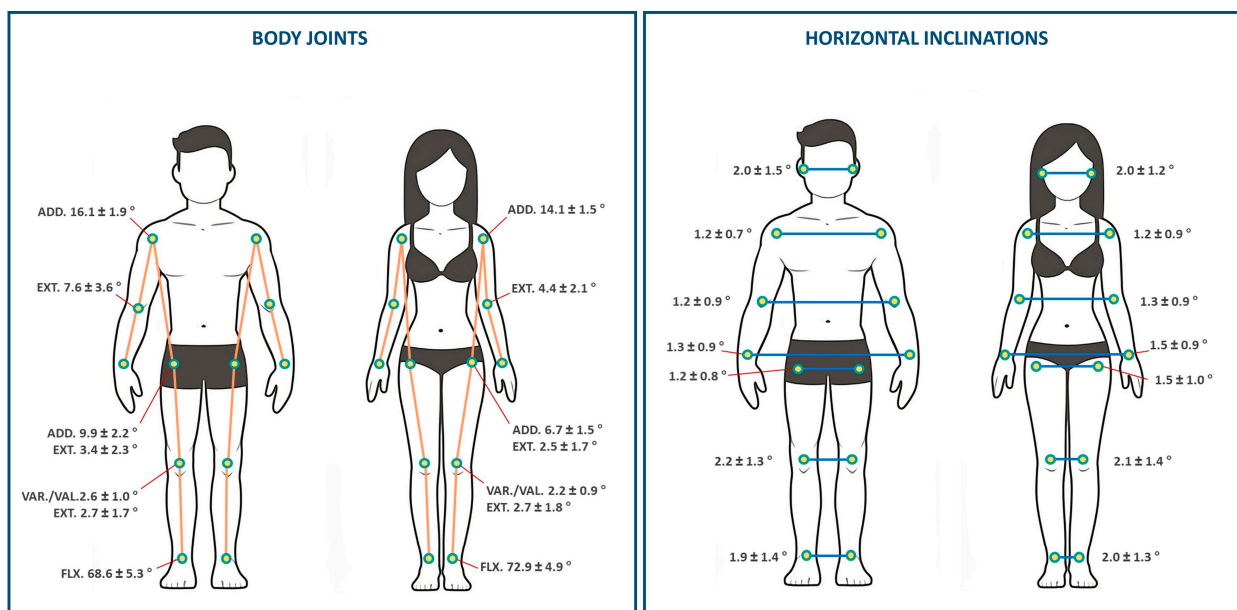


Figure 2. Angle results of the machine learning posture analysis with detailed comparison of body joint angles and horizontal inclinations for men and women, as indicated by mean values \pm standard deviations. (ADD: adduction, EXT: extension, VAR./VAL: varus/valgus, FLX: flexion).

3.1. Test–Retest Reliability

The ICC (3,k) was used to assess the reliability of measurements when repeated on the same sample after a week. Table 1 shows excellent reliability across all measurements, with ICC (3,k) values ranging from 0.67 to 0.95.

3.2. Principal Component Analysis and Clustering Methods

We fed the data into the PCA algorithm and identified four components. To ensure the representation of 90% of the data variance, we focused on the first two main components, which had variance ratio values of 0.815 and 0.093. Both the elbow method and the silhouette

analysis suggested the presence of two cluster groups (CG1, CG2). The majority of clustering algorithms produced similar silhouette scores (approximately 0.55) and cluster divisions. However, the mean-shift method yielded the highest score (0.568), and we therefore adopted its cluster divisions for further analyses, as shown in Figure 3. Inferential statistics were used to analyze the data divided by the mean-shift method (Table 2). The cluster analysis highlighted a significant difference in body vector lengths, particularly in the shoulder–hip difference: CG1 = 57.5 ± 7.0 pd while CG2 = 86.6 ± 10.7 pd, with a large effect size of $d = 3.21$.



Figure 3. Representation of data distribution from the application of the clustering algorithms within the space of the first two principal components.

Table 2. Results of the postural analysis with ML algorithms based on the mean-shift clustering.

	Postural Parameters	Mean \pm SD		Sig.	Effect Size (d)
		CG1	CG2		
Body Joints (°)	Shoulder adduction angle	14.7 \pm 1.6	15.1 \pm 2.2	0.112	0.24
	Elbow extension angle	4.8 \pm 2.6	6.3 \pm 3.4	0.001 **	0.50
	Hip adduction angle	6.5 \pm 1.6	9.4 \pm 2.2	<0.001 ***	1.53
	Hip extension angle	2.5 \pm 1.6	3.2 \pm 2.4	0.035 *	0.36
	Knee varus/valgus angle	2.3 \pm 0.9	2.5 \pm 1.0	0.258	0.19
	Knee extension angle	73.1 \pm 4.7	69.2 \pm 5.5	0.146	−0.24
	Ankle flexion angle	14.7 \pm 1.6	15.1 \pm 2.2	<0.001 ***	−0.78
Horizontal inclinations (°)	Ear line	2.0 \pm 1.2	2.0 \pm 1.4	0.89	−0.02
	Shoulder line	1.3 \pm 0.9	1.1 \pm 0.7	0.032 *	−0.34
	Elbow line	1.3 \pm 1.0	1.2 \pm 0.8	0.591	−0.08
	Wrist line	1.4 \pm 0.9	1.4 \pm 0.9	0.958	−0.01
	Hip line	1.7 \pm 1.0	1.1 \pm 0.8	<0.001 ***	−0.64
	Knee line	2.2 \pm 1.4	2.1 \pm 1.4	0.418	−0.12
	Ankle line	2.0 \pm 1.4	2.0 \pm 1.4	0.822	0.04
Vertical inclinations (°)	Neck inclination	15.5 \pm 3.1	14.0 \pm 3.4	0.006 **	−0.46
	Trunk forward inclination	1.5 \pm 1.1	2.0 \pm 1.4	0.007 **	0.42
	Body imbalance	1.3 \pm 0.6	1.0 \pm 0.4	0.004 **	−0.51
	Leg inclination	1.9 \pm 0.6	1.7 \pm 0.6	0.034 *	−0.31
Vector length (pd)	Shoulder–hip difference	57.5 \pm 7.0	86.6 \pm 10.7	<0.001 ***	3.21
	Torso vector	233.4 \pm 16.2	295.9 \pm 21.6	<0.001 ***	3.28
	Total arm vector	241.2 \pm 14.1	307.7 \pm 23.4	<0.001 ***	3.44
	Total leg vector	342.6 \pm 19.4	400.3 \pm 22.2	<0.001 ***	2.77

CG1 = clustering group 1; CG2 = clustering group 2. SD = standard deviation, pd = pixel distance. Significance levels: * $p < 0.05$, ** $p < 0.01$, *** $p < 0.001$. Cohen's d : >0.50 = medium effect size, >0.80 = large effect size.

4. Discussion

Postural assessment plays a fundamental role in clinical [41], sport [42], and ergonomic evaluation [43]. This study investigated using ML to enhance postural analysis, established normative posture data for healthy men and women, and explored interesting posture patterns using PCA and cluster analysis. Our findings offer insights into the reliability of ML-driven posture analysis and its potential to reveal previously unidentified relationships within postural data.

We expected a significant difference in joint angles and no significant difference in horizontal and vertical inclinations. While postural asymmetries are prevalent in various conditions such as low back pain [44], stroke [45], cerebral palsy [46], Parkinson's disease [47], and scoliosis [48], we recognized that our sample, comprised of healthy participants, would not show substantial asymmetry. These observations differ from our previous work on posture assessment using rasterstereography, where we assessed only the trunk [49]. This difference suggests that the ML approach may be more sensitive in detecting subtle imbalances in healthy individuals. The body angles varied by sex, with a pronounced effect size observed for the shoulder adduction, elbow extension, hip adduction/extension and ankle flexion. In contrast, the knee varus/valgus, hip extension, and neck and trunk inclinations, while statistically significant, exhibited a medium effect size. Men demonstrated higher values of shoulder adduction and elbow extension. However, since these angles influence each other, it is challenging to identify the exact reason for this sex difference. For the neck, a more pronounced inclination was observed in women. This difference, with a medium effect size ($d = -0.55$), could be related to the varied behavior of the neck during daily activities. For example, Tierney et al. [50], found that women have lower neck isometric strength, neck girth, and head mass compared to men when responding to an external force. This subtle difference might influence neck posture, possibly resulting in a generally more forward head position for women.

While some studies have validated already the accuracy of ML algorithms in identifying joint center locations with a precision of 30 mm or less [51,52], the use of ML in assessing human posture is a growing field with limited studies to date. Moreira et al. [53] recently published an article employing a PoseNet API-based method to assess human posture in a sample of 20 adults. Unlike our study, they only calculated the tilt, i.e., horizontal inclination of five anatomical landmarks. They observed a horizontal head tilt of $3.77^\circ \pm 2.92$, shoulder tilt of $2.18^\circ \pm 1.56$, hip tilt of $1.58^\circ \pm 0.86$, ankle tilt of $1.67^\circ \pm 0.98$, right knee tilt of $163.93^\circ \pm 4.03$, and left knee tilt of $165.94^\circ \pm 3.56$. Comparing these results with ours, we noted discrepancies for the head, shoulders, and knee tilts. Notably, their definition of "knee tilt" corresponds to the valgus/varus position of the knee. However, their reported values of approximately $14\text{--}16^\circ$ (obtained by subtracting their results from the flat angle of 180°) seem questionable, as other studies have indicated that a knee angle of -3° or $+3^\circ$ is indicative of a valgus or varus knee, respectively [54,55]. Despite their higher values, the validity of their results is uncertain due to the heterogeneous nature of their sample, ranging from 12 to 66 years old. Our findings for the knee varus/valgus angle align with the neutral range. The lack of similar studies using ML methods for posture analysis makes direct comparisons with existing research challenging. While we found some similarities with two studies using a mobile application, detailed comparisons are difficult [4,56]. These apps rely on specific positions of the body landmarks, whereas human pose estimation algorithms are based on 3D joint center locations [57].

In order to assess the reliability of this method, we tested a sample of participants twice and evaluated the ICC (3,k). We found substantial-to-excellent agreement for both horizontal and vertical inclinations, while measures of the body joints demonstrated excellent agreement. The reliability of MediaPipe has previously been explored in other studies. For example, Ota et al. [58] assessed the reliability using a motion capture system during bilateral squat movements and found ICC scores ranging between 0.92 and 0.96. Saiki et al. [38] conducted two studies on the reliability of their method in patients with knee osteoarthritis. They initially demonstrated excellent test-retest reliability ($\text{ICC}(1, 1) = 1.000$) and substan-

tial agreement with radiography (ICC (2, 1) = 0.915) for measuring the hip–knee–ankle angle. A subsequent study on knee range of motion after total knee arthroplasty further showed high ICC values for knee extension and flexion (ICC = 1.000 for both). Their findings were consistent with both X-ray and goniometry measurements (ICC range: 0.963–0.994) [59]. Also, Latreche et al. [60] confirmed the valid results of MediaPipe for specific rehabilitation movements. They reported ICC values of 0.96, 0.99, 0.99, and 0.99 for shoulder abduction, adduction, extension, and flexion movements, respectively. Furthermore, Hii et al. [61] compared the gait analysis accomplished with MediaPipe and Vicon cameras, finding good-to-excellent ICC agreement in all temporal gait parameters except for double support time, which exhibited an ICC > 0.50.

In this study, we analyzed the length of body vectors. While limited in reflecting real-world measurements, they offer insight into underlying anatomical variations. The magnitude of the correlation coefficients (ranging from 0.473 to 0.60) indicates a moderately strong relationship between height and posture variables. This positive correlation signifies that as height increases, there tends to be a corresponding change in the length of body vectors. As expected, we observed a less pronounced than anticipated shoulder–hip difference between sexes (men: 83.8 ± 14.9 pd; women: 63.4 ± 13.3 pd), aligning with well-established sex differences in body lengths [62]. When we performed cluster analyses, we expected it to primarily differentiate participants based on their sex. However, we found a marked distinction in body vector lengths between the two groups formed by the analysis (CG1 and CG2), and this distinction was independent of the sex of participants. Both groups contained a mix of men and women, demonstrating the ability of the cluster analysis to identify a pattern of posture variation beyond the traditional sex-based anatomical differences. This distinction was much more pronounced than the subtle differences observed for body angles and inclinations within the cluster analysis. Notably, the arm and torso lengths differed between groups: 233.4 ± 16.2 pd (CG1) vs. 295.9 ± 21.6 pd (CG2), with an effect size of 3.28; and 241.2 ± 14.1 pd (CG1) vs. 307.7 ± 23.4 pd (CG2), with an effect size of 3.44. The most prominent difference influencing PCA was the shoulder–hip differential: 57.5 ± 7.0 pd (CG1) vs. 86.6 ± 10.7 pd (CG2), with an effect size of 3.21. This difference highlights two distinct postural types similar to the somatotype classification. Olds et al. [63] utilized 3D anthropometry with 301 adults to identify body shape clusters, aligning their findings with traditional somatotype classifications [64], i.e., endomorphic: larger widths, shorter limbs; ectomorphic: longer limbs, narrower hips. Our study followed a different approach, employing an unsupervised ML method to discern two distinct postural categories. However, these categories appear to echo the somatotype trends: CG1 includes individuals with shorter body segments and similar shoulder and hip widths; CG2 includes individuals with longer body segments with notably wider shoulders compared to hips.

This data-driven approach offers a novel perspective on postural assessment. Our findings highlight the potential of ML models to provide fast, reliable posture analysis. In clinical scenarios, this could enhance the understanding of anatomical variations, support personalized interventions in physical therapy and ergonomics, potentially aid preventive screening, and help define the boundaries between correctable and pathological posture. Furthermore, it could help coaches evaluate the effectiveness of athletic movements [65], optimize training, and prevent posture-related injuries [66,67]. Requiring minimal clothing removal, this ML-based method reduces subjectivity in traditional postural analysis and could guide physiotherapy, remote rehabilitation, and pathology management [68,69]. Additionally, the use of PCA and clustering suggests that posture classification may be possible regardless of sex. While cluster analysis provides valuable insights into sport tactics [70], its application to athletes' posture data may represent an innovative approach. This could help identify physiological characteristics closely linked to specific sports, revealing how aspects of the human body directly impact athletic performance.

This research presents certain limitations. First, our analysis focused on a homogenous sample. While we found significant differences, a more diverse population with a wider age

range (e.g., 40–70) could yield more robust findings and highlight age-specific conditions, as well as highlighting any age-specific postural differences. Second, requiring a specific posture for the photos might potentially obscure certain postural alterations. Future research should encompass a broader demographic to highlight more generalizable postural conditions, as well as the analysis of dynamic postures. Furthermore, this approach should be tested in the context of specific musculoskeletal disorders, e.g., lower back pain, and other orthopedic or neurological conditions.

5. Conclusions

This study introduces a novel ML approach with significant clinical potential for postural analysis, offering distinct classification and reduced subjectivity. This efficient, non-invasive method could enhance personalized treatment in physical therapy and ergonomics. Our research confirms its applicability and reliability in assessing healthy adult posture, providing normative data. We identified highly reliable postural parameters and highlighted sex-related differences. Importantly, cluster analysis revealed postural characteristics independent of sex, such as limb length and shoulder–hip width differences. These findings suggest potential new opportunities for ML-driven posture classification.

Author Contributions: Conceptualization, F.R., S.D.G. and G.M.; methodology, F.R. and S.D.G.; software, F.R. and S.D.G.; validation, S.C.; formal analysis, F.R. and S.D.G.; investigation, F.R. and G.M.; resources, G.M.; data curation, D.F., S.C. and G.M.; writing—original draft preparation, F.R., S.C. and G.M.; writing—review and editing, D.F.; visualization, F.R.; supervision, D.F. and G.M.; project administration, G.M.; funding acquisition, G.M. All authors have read and agreed to the published version of the manuscript.

Funding: This study was funded by the Italian Ministry of University and Research (MUR) (grant number PRIN 2022PZH8SX). The funder played no role in study design, data collection, analysis and interpretation of data, or the writing of this manuscript.

Institutional Review Board Statement: This study was conducted in accordance with the Declaration of Helsinki and approved by the Institutional Review Board of the Research Center on Motor Activities (CRAM) (Protocol n.: CRAM-035-2023, 15 March 2023).

Informed Consent Statement: Signed informed consent was obtained from all subjects involved in the study.

Data Availability Statement: The datasets used and/or analyzed during the current study are available from the corresponding author on reasonable request.

Conflicts of Interest: All authors declare no financial or non-financial competing interests.

Appendix A

Table A1. Explanation of how each postural parameter is calculated based on the keypoints.

Postural Parameter	Function Calculation
Body joints (°)	
Shoulder abduction/adduction angle	Angle between the hip, shoulder and elbow keypoints +.
Elbow flexion/extension angle	Angle between the shoulder, elbow and wrist keypoints +.
Hipabduction/adduction angle	Angle between the shoulder, hip and knee keypoints +.
Kneevarus/valgus angle	Angle between the hip, knee and ankle keypoints +.
Hip flexion/extension angle	Angle between the shoulder, hip and knee keypoints ++.
Knee flexion/extension angle	Angle between the hip, knee and ankle keypoints ++.

Table A1. Cont.

Postural Parameter	Function Calculation
Ankle flexion/extension angle	Angle between the knee, ankle and foot index keypoints ++.
Horizontal inclinations (°)	
Ears line	Angle between an horizontal vector passing for one keypoint and a vector connecting the two ears keypoints +.
Shoulders line	Angle between an horizontal vector passing for one keypoint and a vector connecting the two shoulders keypoints +.
Elbows line	Angle between an horizontal vector passing for one keypoint and a vector connecting the two elbows keypoints +.
Wrists line	Angle between an horizontal vector passing for one keypoint and a vector connecting the two wrists keypoints +.
Hips line	Angle between an horizontal vector passing for one keypoint and a vector connecting the two hips keypoints +.
Knees line	Angle between an horizontal vector passing for one keypoint and a vector connecting the two knees keypoints +.
Ankles line	Angle between an horizontal vector passing for one keypoint and a vector connecting the two ankles keypoints +.
Vertical inclinations (°)	
Neck inclination	Angle between a vertical vector passing for the shoulders midpoint and a vector connecting the shoulders and ears midpoints ++.
Trunk forward inclination	Angle between a vertical vector passing for the hips midpoint and a vector connecting the hip and shoulder midpoints ++.
Body imbalance	Angle between a vertical vector passing for the hips midpoint and a vector connecting the hip and shoulder midpoints +.
Leg inclination	Angle between a vertical vector passing for one keypoint and a vector connecting the hip and knee keypoints ++.
Vectors length (pds)	
Shoulders-hips difference	Difference between the vector connecting the two shoulders and the two hips keypoints +.
Torso vector	Length of the vector connecting the hip and shoulder keypoints +.
Total arm vector	Sum of the upper and lower arm vectors.
Total leg vector	Sum of the thigh and shank vectors.

pd = pixel distance, + front and back photos, ++ lateral photos.

References

1. Ferreira, M.L.; de Luca, K.; Haile, L.M.; Steinmetz, J.D.; Culbreth, G.T.; Cross, M.; A Kopec, J.; Ferreira, P.H.; Blyth, F.M.; Buchbinder, R.; et al. Global, regional, and national burden of low back pain, 1990–2020, its attributable risk factors, and projections to 2050: A systematic analysis of the Global Burden of Disease Study 2021. *Lancet Rheumatol.* **2023**, *5*, e316–e329. [[CrossRef](#)] [[PubMed](#)]
2. Roggio, F.; Ravalli, S.; Maugeri, G.; Bianco, A.; Palma, A.; Di Rosa, M.; Musumeci, G. Technological advancements in the analysis of human motion and posture management through digital devices. *World J. Orthop.* **2021**, *12*, 467–484. [[CrossRef](#)] [[PubMed](#)]
3. Corazza, S.; Mündermann, L.; Gambaretto, E.; Ferrigno, G.; Andriacchi, T.P. Markerless Motion Capture through Visual Hull, Articulated ICP and Subject Specific Model Generation. *Int. J. Comput. Vis.* **2010**, *87*, 156–169. [[CrossRef](#)]
4. Trovato, B.; Roggio, F.; Sortino, M.; Zanghi, M.; Petrigna, L.; Giuffrida, R.; Musumeci, G. Postural Evaluation in Young Healthy Adults through a Digital and Reproducible Method. *J. Funct. Morphol. Kinesiol.* **2022**, *7*, 98. [[CrossRef](#)]
5. Belli, G.; Toselli, S.; Mauro, M.; Maietta Latessa, P.; Russo, L. Relation between Photogrammetry and Spinal Mouse for Sagittal Imbalance Assessment in Adolescents with Thoracic Kyphosis. *J. Funct. Morphol. Kinesiol.* **2023**, *8*, 68. [[CrossRef](#)] [[PubMed](#)]
6. Phinyomark, A.; Petri, G.; Ibáñez-Marcelo, E.; Osis, S.T.; Ferber, R. Analysis of Big Data in Gait Biomechanics: Current Trends and Future Directions. *J. Med. Biol. Eng.* **2018**, *38*, 244–260. [[CrossRef](#)] [[PubMed](#)]

7. Begg, R.; Kamruzzaman, J. Neural networks for detection and classification of walking pattern changes due to ageing. *Australas. Phys. Eng. Sci. Med.* **2006**, *29*, 188–195. [[CrossRef](#)] [[PubMed](#)]
8. Wahid, F.; Begg, R.K.; Hass, C.J.; Halgamuge, S.; Ackland, D.C. Classification of Parkinson's Disease Gait Using Spatial-Temporal Gait Features. *IEEE J. Biomed. Health Inform.* **2015**, *19*, 1794–1802. [[CrossRef](#)]
9. Lau, H.-y.; Tong, K.-y.; Zhu, H. Support vector machine for classification of walking conditions of persons after stroke with dropped foot. *Hum. Mov. Sci.* **2009**, *28*, 504–514. [[CrossRef](#)]
10. Laroche, D.; Tolambiya, A.; Morisset, C.; Maillefert, J.F.; French, R.M.; Ornetti, P.; Thomas, E. A classification study of kinematic gait trajectories in hip osteoarthritis. *Comput. Biol. Med.* **2014**, *55*, 42–48. [[CrossRef](#)]
11. Zhang, Z.; Hong, R.; Lin, A.; Su, X.; Jin, Y.; Gao, Y.; Peng, K.; Li, Y.; Zhang, T.; Zhi, H.; et al. Automated and accurate assessment for postural abnormalities in patients with Parkinson's disease based on Kinect and machine learning. *J. Neuroeng. Rehabil.* **2021**, *18*, 169. [[CrossRef](#)] [[PubMed](#)]
12. Dindorf, C.; Ludwig, O.; Simon, S.; Becker, S.; Fröhlich, M. Machine Learning and Explainable Artificial Intelligence Using Counterfactual Explanations for Evaluating Posture Parameters. *Bioengineering* **2023**, *10*, 511. [[CrossRef](#)] [[PubMed](#)]
13. Fedorak, C.; Ashworth, N.; Marshall, J.; Paull, H. Reliability of the Visual Assessment of Cervical and Lumbar Lordosis: How Good Are We? *Spine* **2003**, *28*, 1857–1859. [[CrossRef](#)] [[PubMed](#)]
14. Guan, S.Y.; Zheng, J.X.; Sam, N.B.; Xu, S.; Shuai, Z.; Pan, F. Global burden and risk factors of musculoskeletal disorders among adolescents and young adults in 204 countries and territories, 1990–2019. *Autoimmun. Rev.* **2023**, *22*, 103361. [[CrossRef](#)] [[PubMed](#)]
15. Bazarevsky, V.; Grishchenko, I.; Raveendran, K.; Zhu, T.; Zhang, F.; Grundmann, M. BlazePose: On-device real-time body pose tracking. *arXiv* **2020**, arXiv:2006.10204.
16. Cao, Z.; Simon, T.; Wei, S.-E.; Sheikh, Y. Realtime multi-person 2d pose estimation using part affinity fields. In Proceedings of the IEEE Conference on Computer Vision and Pattern Recognition, Honolulu, HI, USA, 21–26 July 2017; pp. 7291–7299.
17. Abadi, M.; Agarwal, A.; Barham, P.; Brevdo, E.; Chen, Z.; Citro, C.; Corrado, G.S.; Davis, A.; Dean, J.; Devin, M. Tensorflow: Large-scale machine learning on heterogeneous distributed systems. *arXiv* **2016**, arXiv:1603.04467.
18. Papandreou, G.; Zhu, T.; Kanazawa, N.; Toshev, A.; Tompson, J.; Bregler, C.; Murphy, K. Towards accurate multi-person pose estimation in the wild. In Proceedings of the IEEE Conference on Computer Vision and Pattern Recognition, Honolulu, HI, USA, 21–26 July 2017; pp. 4903–4911.
19. Güneş, G.; Jansen, T.S.; Dill, S.; Schulz, J.B.; Dafotakis, M.; Hoog Antink, C.; Braczynski, A.K. Video-Based Hand Movement Analysis of Parkinson Patients before and after Medication Using High-Frame-Rate Videos and MediaPipe. *Sensors* **2022**, *22*, 7992. [[CrossRef](#)] [[PubMed](#)]
20. Du, Q.; Bai, H.; Zhu, Z. Intelligent Evaluation Method of Human Cervical Vertebra Rehabilitation Based on Computer Vision. *Sensors* **2023**, *23*, 3825. [[CrossRef](#)]
21. Fernández, M.M.; Fernández, J.Á.; Bajo, J.M.; Delrieux, C. Ergonomic risk assessment based on computer vision and machine learning. *Comput. Ind. Eng.* **2020**, *149*, 106816.
22. Binish Zahra, S.; Adnan Khan, M.; Abbas, S.; Masood Khan, K.; Al Ghamdi, M.A.; Almotiri, S.H. Marker-based and Marker-less Motion Capturing Video Data: Person & Activity Identification Comparison Based on Machine Learning Approaches. *Comput. Mater. Contin.* **2021**, *66*, 1269–1282. [[CrossRef](#)]
23. Kaur, R.; Motl, R.W.; Sowers, R.; Hernandez, M.E. A Vision-Based Framework for Predicting Multiple Sclerosis and Parkinson's Disease Gait Dysfunctions-A Deep Learning Approach. *IEEE J. Biomed. Health Inform.* **2023**, *27*, 190–201. [[CrossRef](#)]
24. Lugaresi, C.; Tang, J.; Nash, H.; McClanahan, C.; Uboweja, E.; Hays, M.; Zhang, F.; Chang, C.-L.; Yong, M.G.; Lee, J. Mediapipe: A framework for building perception pipelines. *arXiv* **2019**, arXiv:1906.08172.
25. Singhal, R.; Modi, H.; Srihari, S.; Gandhi, A.; Prakash, C.O.; Eswaran, S. Body Posture Correction and Hand Gesture Detection Using Federated Learning and Mediapipe. In Proceedings of the 2023 2nd International Conference for Innovation in Technology (INOCON), Bangalore, India, 3–5 March 2023; pp. 1–6.
26. Grishchenko, I.; Bazarevsky, V.; Bazavan, E.G.; Na, L.; Mayes, J. 3D Pose Detection with MediaPipe BlazePose GHUM and TensorFlow.js. Available online: <https://blog.tensorflow.org/2021/08/3d-pose-detection-with-mediapipe-blazepose-ghum-tfjs.html> (accessed on 25 March 2024).
27. Lafayette, T.B.d.G.; Kunst, V.H.d.L.; Melo, P.V.d.S.; Guedes, P.d.O.; Teixeira, J.M.X.N.; Vasconcelos, C.R.d.; Teichrieb, V.; da Gama, A.E.F. Validation of Angle Estimation Based on Body Tracking Data from RGB-D and RGB Cameras for Biomechanical Assessment. *Sensors* **2023**, *23*, 3. [[CrossRef](#)]
28. Das, K.; de Paula Oliveira, T.; Newell, J. Comparison of markerless and marker-based motion capture systems using 95% functional limits of agreement in a linear mixed-effects modelling framework. *Sci. Rep.* **2023**, *13*, 22880. [[CrossRef](#)]
29. Supanich, W.; Kulkarineetham, S.; Sukphokha, P.; Wisarnart, P. Machine Learning-Based Exercise Posture Recognition System Using MediaPipe Pose Estimation Framework. In Proceedings of the 2023 9th International Conference on Advanced Computing and Communication Systems (ICACCS), Coimbatore, India, 17–18 March 2023; pp. 2003–2007.
30. Lin, Y.; Jiao, X.; Zhao, L. Detection of 3D Human Posture Based on Improved Mediapipe. *J. Comput. Commun.* **2023**, *11*, 102–121. [[CrossRef](#)]
31. Federolf, P.; Tecante, K.; Nigg, B. A holistic approach to study the temporal variability in gait. *J. Biomech.* **2012**, *45*, 1127–1132. [[CrossRef](#)] [[PubMed](#)]

32. Federolf, P.A.; Boyer, K.A.; Andriacchi, T.P. Application of principal component analysis in clinical gait research: Identification of systematic differences between healthy and medial knee-osteoarthritic gait. *J. Biomech.* **2013**, *46*, 2173–2178. [[CrossRef](#)] [[PubMed](#)]
33. Federolf, P.A. A novel approach to study human posture control: “Principal movements” obtained from a principal component analysis of kinematic marker data. *J. Biomech.* **2016**, *49*, 364–370. [[CrossRef](#)]
34. Pradhan, G.; Prabhakaran, B. Clustering of human motions based on feature-level fusion of multiple body sensor data. In Proceedings of the 1st ACM International Health Informatics Symposium, Arlington, VA, USA, 11–12 November 2010; pp. 66–75.
35. Hermez, L.; Halimi, A.; Houmani, N.; Garcia-Salicetti, S.; Galarraga, O.; Vigneron, V. Clinical Gait Analysis: Characterizing Normal Gait and Pathological Deviations Due to Neurological Diseases. *Sensors* **2023**, *23*, 6566. [[CrossRef](#)]
36. Sidarta, A.; Komar, J.; Ostry, D.J. Clustering analysis of movement kinematics in reinforcement learning. *J. Neurophysiol.* **2022**, *127*, 341–353. [[CrossRef](#)]
37. Emery, C.A. Considering cluster analysis in sport medicine and injury prevention research. *Clin. J. Sport. Med.* **2007**, *17*, 211–214. [[CrossRef](#)] [[PubMed](#)]
38. Saiki, Y.; Kabata, T.; Ojima, T.; Kajino, Y.; Kubo, N.; Tsuchiya, H. Reliability and validity of pose estimation algorithm for measurement of knee range of motion after total knee arthroplasty. *Bone Jt. Res.* **2023**, *12*, 313–320. [[CrossRef](#)] [[PubMed](#)]
39. Kendall, F.P.; McCreary, E.K.; Provance, P.G.; Crosby, R.W.; Andrews, P.J.; Krause, C. *Muscles, Testing and Function: With Posture and Pain*, 4th ed.; Lippincott Williams & Wilkins: Philadelphia, PA, USA, 1993.
40. Bazarevsky, V.; Grishchenko, I. On-Device, Real-Time Body Pose Tracking with MediaPipe BlazePose. Available online: <https://blog.research.google/2020/08/on-device-real-time-body-pose-tracking.html> (accessed on 25 March 2024).
41. Smart, L.J., Jr.; Smith, D.L. Postural dynamics: Clinical and empirical implications. *J. Manip. Physiol. Ther.* **2001**, *24*, 340–349. [[CrossRef](#)] [[PubMed](#)]
42. Andreeva, A.; Melnikov, A.; Skvortsov, D.; Akhmerova, K.; Vavaev, A.; Golov, A.; Draugelite, V.; Nikolaev, R.; Chechelniciaia, S.; Zhuk, D. Postural stability in athletes: The role of sport direction. *Gait Posture* **2021**, *89*, 120–125. [[CrossRef](#)] [[PubMed](#)]
43. Ray, S.J.; Teizer, J. Real-time construction worker posture analysis for ergonomics training. *Adv. Eng. Inform.* **2012**, *26*, 439–455. [[CrossRef](#)]
44. Yu, Q.; Huang, H.; Zhang, Z.; Hu, X.; Li, W.; Li, L.; Chen, M.; Liang, Z.; Lo, W.L.A.; Wang, C. The association between pelvic asymmetry and non-specific chronic low back pain as assessed by the global postural system. *BMC Musculoskelet. Disord.* **2020**, *21*, 596. [[CrossRef](#)] [[PubMed](#)]
45. Tasseel-Ponche, S.; Yelnik, A.P.; Bonan, I.V. Motor strategies of postural control after hemispheric stroke. *Neurophysiol. Clin.* **2015**, *45*, 327–333. [[CrossRef](#)] [[PubMed](#)]
46. Holmes, C.; Brock, K.; Morgan, P. Postural asymmetry in non-ambulant adults with cerebral palsy: A scoping review. *Disabil. Rehabil.* **2019**, *41*, 1079–1088. [[CrossRef](#)]
47. Beretta, V.S.; Barbieri, F.A.; Orcioli-Silva, D.; Dos Santos, P.C.R.; Simieli, L.; Vitório, R.; Gobbi, L.T.B. Can Postural Control Asymmetry Predict Falls in People With Parkinson’s Disease? *Motor Control* **2018**, *22*, 449–461. [[CrossRef](#)]
48. Prowse, A.; Pope, R.; Gerdhem, P.; Abbott, A. Reliability and validity of inexpensive and easily administered anthropometric clinical evaluation methods of postural asymmetry measurement in adolescent idiopathic scoliosis: A systematic review. *Eur. Spine J.* **2016**, *25*, 450–466. [[CrossRef](#)]
49. Roggio, F.; Petrigna, L.; Trovato, B.; Zanghì, M.; Sortino, M.; Vitale, E.; Rapisarda, L.; Testa, G.; Pavone, V.; Pavone, P.; et al. Thermography and rasterstereography as a combined infrared method to assess the posture of healthy individuals. *Sci. Rep.* **2023**, *13*, 4263. [[CrossRef](#)] [[PubMed](#)]
50. Tierney, R.T.; Sitler, M.R.; Swanik, C.B.; Swanik, K.A.; Higgins, M.; Torg, J. Gender differences in head-neck segment dynamic stabilization during head acceleration. *Med. Sci. Sports Exerc.* **2005**, *37*, 272–279. [[CrossRef](#)] [[PubMed](#)]
51. Nakano, N.; Sakura, T.; Ueda, K.; Omura, L.; Kimura, A.; Iino, Y.; Fukashiro, S.; Yoshioka, S. Evaluation of 3D Markerless Motion Capture Accuracy Using OpenPose With Multiple Video Cameras. *Front. Sports Act. Living* **2020**, *2*, 50. [[CrossRef](#)] [[PubMed](#)]
52. Zago, M.; Luzzago, M.; Marangoni, T.; De Cecco, M.; Tarabini, M.; Galli, M. 3D Tracking of Human Motion Using Visual Skeletonization and Stereoscopic Vision. *Front. Bioeng. Biotechnol.* **2020**, *8*, 181. [[CrossRef](#)] [[PubMed](#)]
53. Moreira, R.; Fialho, R.; Teles, A.S.; Bordalo, V.; Vasconcelos, S.S.; Gouveia, G.P.d.M.; Bastos, V.H.; Teixeira, S. A computer vision-based mobile tool for assessing human posture: A validation study. *Comput. Methods Programs Biomed.* **2022**, *214*, 106565. [[CrossRef](#)] [[PubMed](#)]
54. Shelton, T.J.; Nedopil, A.J.; Howell, S.M.; Hull, M.L. Do varus or valgus outliers have higher forces in the medial or lateral compartments than those which are in-range after a kinematically aligned total knee arthroplasty? limb and joint line alignment after kinematically aligned total knee arthroplasty. *Bone Jt. J.* **2019**, *101*, 1319. [[CrossRef](#)]
55. Bellemans, J.; Colyn, W.; Vandenuecker, H.; Victor, J. The Chitranjan Ranawat award: Is neutral mechanical alignment normal for all patients? The concept of constitutional varus. *Clin. Orthop. Relat. Res.* **2012**, *470*, 45–53. [[CrossRef](#)]
56. Hopkins, B.B.; Vehrs, P.R.; Fellingham, G.W.; George, J.D.; Hager, R.; Ridge, S.T. Validity and Reliability of Standing Posture Measurements Using a Mobile Application. *J. Manip. Physiol. Ther.* **2019**, *42*, 132–140. [[CrossRef](#)] [[PubMed](#)]
57. Needham, L.; Evans, M.; Cosker, D.P.; Wade, L.; McGuigan, P.M.; Bilzon, J.L.; Colyer, S.L. The accuracy of several pose estimation methods for 3D joint centre localisation. *Sci. Rep.* **2021**, *11*, 20673. [[CrossRef](#)] [[PubMed](#)]
58. Ota, M.; Tateuchi, H.; Hashiguchi, T.; Kato, T.; Ogino, Y.; Yamagata, M.; Ichihashi, N. Verification of reliability and validity of motion analysis systems during bilateral squat using human pose tracking algorithm. *Gait Posture* **2020**, *80*, 62–67. [[CrossRef](#)]

59. Saiki, Y.; Kabata, T.; Ojima, T.; Kajino, Y.; Inoue, D.; Ohmori, T.; Yoshitani, J.; Ueno, T.; Yamamuro, Y.; Taninaka, A.; et al. Reliability and validity of OpenPose for measuring hip-knee-ankle angle in patients with knee osteoarthritis. *Sci. Rep.* **2023**, *13*, 3297. [[CrossRef](#)]
60. Latreche, A.; Kelaiaia, R.; Chemori, A.; Kerboua, A. Reliability and validity analysis of MediaPipe-based measurement system for some human rehabilitation motions. *Measurement* **2023**, *214*, 112826. [[CrossRef](#)]
61. Hii, C.S.T.; Gan, K.B.; Zainal, N.; Mohamed Ibrahim, N.; Azmin, S.; Mat Desa, S.H.; van de Warrenburg, B.; You, H.W. Automated Gait Analysis Based on a Marker-Free Pose Estimation Model. *Sensors* **2023**, *23*, 6489. [[CrossRef](#)] [[PubMed](#)]
62. Jungers, W.L.; Falsetti, A.B.; Wall, C.E. Shape, relative size, and size-adjustments in morphometrics. *Am. J. Phys. Anthropol.* **1995**, *38*, 137–161. [[CrossRef](#)]
63. Olds, T.; Daniell, N.; Petkov, J.; David Stewart, A. Somatotyping using 3D anthropometry: A cluster analysis. *J. Sports Sci.* **2013**, *31*, 936–944. [[CrossRef](#)] [[PubMed](#)]
64. Carter, J.E.L.; Heath, B.H. *Somatotyping: Development and Applications*; Cambridge University Press: Cambridge, UK, 1990.
65. Li, Y.C.; Chang, C.T.; Cheng, C.C.; Huang, Y.L. Baseball Swing Pose Estimation Using OpenPose. In Proceedings of the 2021 IEEE International Conference on Robotics, Automation and Artificial Intelligence (RAAI), Hong Kong, China, 21–23 April 2021; pp. 6–9.
66. Henriquez, M.; Sumner, J.; Faherty, M.; Sell, T.; Bent, B. Machine Learning to Predict Lower Extremity Musculoskeletal Injury Risk in Student Athletes. *Front. Sports Act. Living* **2020**, *2*, 576655. [[CrossRef](#)] [[PubMed](#)]
67. Giustino, V.; Messina, G.; Patti, A.; Padua, E.; Zangla, D.; Drid, P.; Battaglia, G.; Palma, A.; Bianco, A. Effects of a Postural Exercise Program on Vertical Jump Height in Young Female Volleyball Players with Knee Valgus. *Int. J. Environ. Res. Public Health* **2022**, *19*, 3953. [[CrossRef](#)] [[PubMed](#)]
68. Kishore, D.M.; Bindu, S.; Manjunath, N.K. Estimation of Yoga Postures Using Machine Learning Techniques. *Int. J. Yoga* **2022**, *15*, 137–143. [[CrossRef](#)] [[PubMed](#)]
69. Chua, J.; Ong, L.-Y.; Leow, M.-C. Telehealth Using PoseNet-Based System for In-Home Rehabilitation. *Future Internet* **2021**, *13*, 173. [[CrossRef](#)]
70. Anil Duman, E.; Sennaroğlu, B.; Tuzkaya, G. A cluster analysis of basketball players for each of the five traditionally defined positions. *Proc. Inst. Mech. Eng. Part. P J. Sports Eng. Technol.* **2024**, *238*, 55–75. [[CrossRef](#)]

Disclaimer/Publisher's Note: The statements, opinions and data contained in all publications are solely those of the individual author(s) and contributor(s) and not of MDPI and/or the editor(s). MDPI and/or the editor(s) disclaim responsibility for any injury to people or property resulting from any ideas, methods, instructions or products referred to in the content.